

EXPERIMENTAL DETERMINATION OF INTERFACE SHEAR STRESSES SIMULATING THE MIDSPAN AREA OF CONCRETE SLABS POST- STRENGTHENED WITH CFRP STRIPS

Karsten Schilde, University of Kassel, Germany

Werner Seim, University of Kassel, Germany

Heiko Engelhard, University of Kassel, Germany

Abstract

A test set-up for studying bond failure between concrete surface and laminate will be presented. With this new test set-up it is possible to simulate geometrical and mechanical conditions between two cracks of a post-strengthened concrete slab. For this purpose two jacks are fixed between a concrete-block and two anchorage-bodies. A separate control of the two jacks makes it possible to vary the gradient of shear stresses, which have to be transmitted between composite and concrete. All this takes into consideration that debonding always starts in a section where high shear forces and high bending moments exist.

The dimensions of the concrete-block have been obtained from various full scale tests carried out on CFRP strengthened slabs. In a first series, 7 bonding tests were carried out. The results of the interface shear tests will be compared to the results of finite-element calculations.

Keywords: post-strengthening; CFRP; debonding; concrete; slab; beam.

Introduction

Steel-plates have been used since the end of the 1960s to increase the load-bearing capacity of concrete-structures. Numerous theoretical and experimental studies have led to capable guidelines for the post-strengthening of slabs and beams (e.g. [1]). These theories assume that stress peaks at the plate end initiate bond failure. The stress peaks are induced by the eccentricity of tension forces at the end of the steel-plates.

Post-strengthening with CFRP-strips has been in use since the 1990s. Those strips are much thinner than steel-plates. Therefore, the stresses resulting from the distance between tension force in the laminate and the adhesive and concrete surface respectively are negligibly small.

Nevertheless, even for CFRP-strips all previous studies and tests concerning bond failure were restricted to the situation at the end of the laminate (compare figure 1, A). But various tests ([2], [3], [4]) have shown that failure of concrete slabs strengthened by the use of externally bonded CFRP strips always starts in a section where high shear forces and high bending-moments exist (see figure 1, B). Failure occurs as debonding of laminate from concrete surface. Stress peaks at flexural cracks and shear cracks respectively can be identified as responsible for debonding. A vertical relative displacement between crack surfaces seems to be of relevance, because supplementary normal stresses between laminate and concrete surface are induced.

A series of tests has been carried out to study the development of shear stresses between CFRP-strip and concrete surface as well as failure loads and failure modes in a section between two cracks (figure 1, B). Therefore design and construction of a new test set-up was necessary.

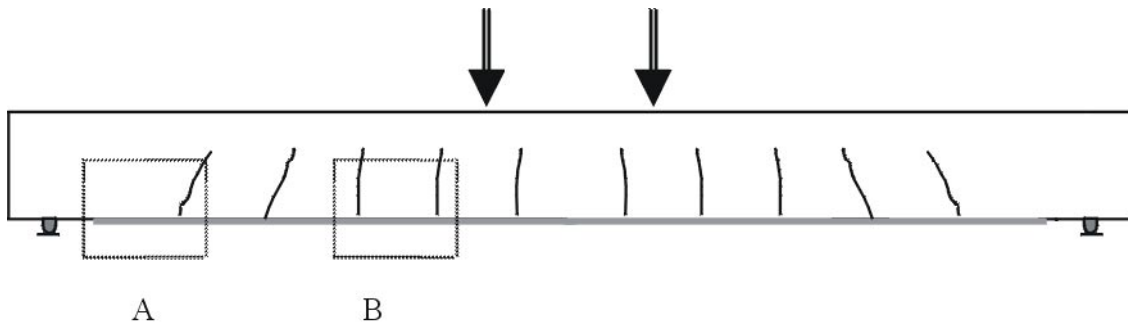


Figure 1. Bending member strengthened with FRP

Test Set-Up and Loading Procedure

Test Set-Up

The test set-up (see figure 2) consists of the concrete-block with two bonded laminates, two jacks and two anchorage-bodies. In order to use the anchorage-bodies repeatedly, they were made of steel instead of concrete.

The laminates are clamped to the anchorage-bodies by contact pressure. Preliminary tests have shown that the contact pressure is sufficient and that a slip of a laminate out of the anchorage-body in the range of the forces brought up during the tests does not affect the outcome.

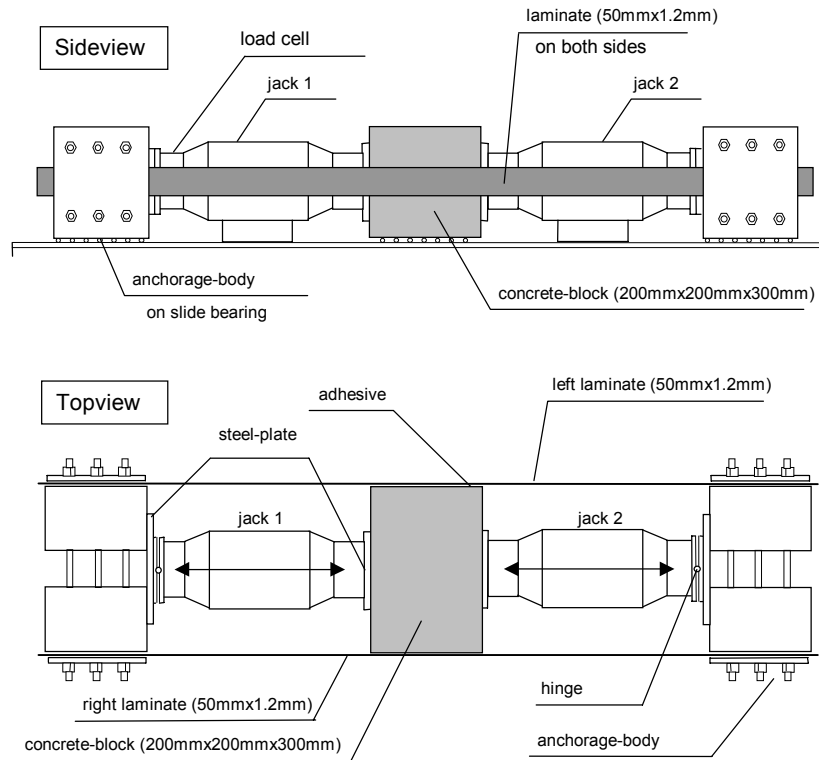


Figure 2. Test set-up

In 1998, 14 full-scale slabs post strengthened by use of CFRP-strips were tested at the University of California, San Diego [2]. Crack distances for these tests lay between 75 and 330 mm. Close to the centre of the slabs, crack distances resided between 180 and 230 mm. Results of calculations based on equations for admitting crack widths [5] showed similar values. For the first series of anchoring tests, 200 mm were chosen for the length of the concrete-block to represent the crack distance.

Materials

Concrete. The concrete-blocks had dimensions of 200mm/300mm/200mm. Compression strength after 113 days reached values between 42,4 N/mm² and 56,3 N/mm². The mean value was 47,7 N/mm².

CFRP-strips. *S&P Laminates CFK 150/200* (width: 50mm; thickness: 1,2 mm) from the “S&P Clever Reinforcement Company” were used. Young’s Modulus of 164000 N/mm² and a tensile strength of 2700 – 3000 N/mm² were taken from product information.

Adhesive. The CFRP-strips were bonded to the concrete after sandblasting of the concrete surface. *Ispo concretin SK 41* was used as an adhesive. The Young’s Modulus is indicated with 11000 N/mm², the compressive strength with ≥ 100 N/mm² and the bending tensile strength with ≥ 30 N/mm² [6].

Loading Procedure

Figure 3a shows the forces acting at a section between two adjacent cracks of a post-strengthened slab. Figure 3b shows the development of the tension-force resulting from the bending moment for steel-reinforcement and laminate. Before the steel-reinforcement yields, the split of the increasing tension-force depends on the stiffness and the inner lever arm of the laminate and the steel reinforcement (see figure 3b). After steel-yielding, the laminate has to admit the whole part of the increasing tension-force. Pre-strains in the steel reinforcement are not considered in figure 3b. Looking at the tension-forces of the laminate at the two crack surfaces A and B (see figure 4a) the difference of the laminate forces ΔF_l is small up to the point when the steel finally yields. After steel-yielding the laminate forces increase significantly and consequently the difference of the forces ΔF_l , too.

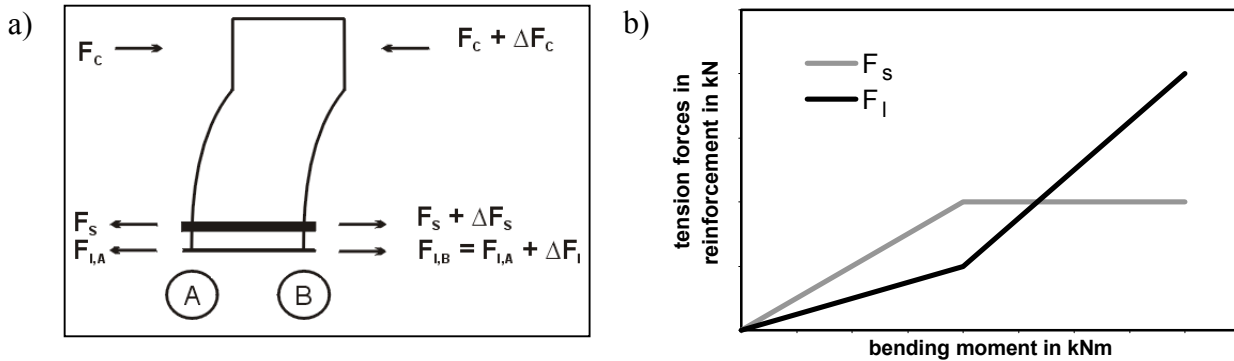


Figure 3. a) Forces at two crack surfaces A and B
b) Development of the tension forces F_l and F_s for increasing bending moment

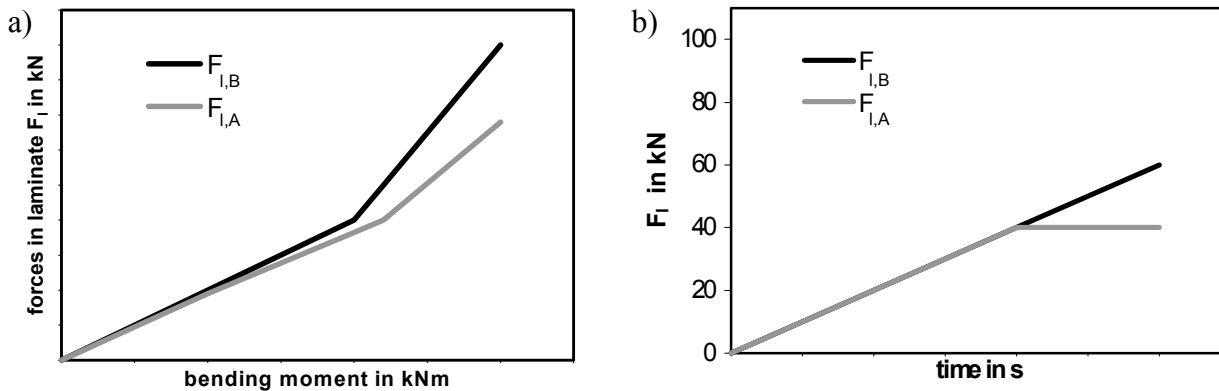


Figure 4. a) Development of tension forces $F_{l,A}$ and $F_{l,B}$
b) Simplified loading procedure at test

For testing purposes, the small difference ΔF_l before steel-yielding can be neglected. With both jacks, forces up to 80 kN were brought up. This means that each laminate took 40 kN tension force. Then the load of jack 1 was increased until failure, whereas the load of jack 2 was held constant

(compare figure 4b). Strain-gauges, fixed on the CFRP-strips, made it possible to calculate the tension forces in the two laminates (see table 1).

In the first series, eight specimens were tested. One end-anchorage test and seven bonding tests simulating the midspan area of a slab were carried out. Test ZRE 0-1 was the first test simulating a section of a concrete slab between two cracks. Therefore, the forces in the two jacks were raised up only to a force of 60 kN before the additional force ΔF_1 was brought up

For tests ZRE 1-1, ZRE 1-2, ZRE 1-3, ZRE 1-5 and ZRE 1-6 the forces in both jacks were increased to 80 kN instead of 60 kN. Specimen ZRE 1-4 was tested with a cyclic load. In ten cycles both forces were increased from 0 kN up to 70 kN. After that, the loading procedure was the same as it was for test ZRE 1-1.

Test Results

Table 1 shows the maximum and minimum forces in the left and the right laminate. As mentioned before, no strain gauges were used for test ZRE 0-1. Therefore the forces in test ZRE 0-1 were equally divided between the two laminates. For the other tests the forces were calculated according to the measured strains. At test ZRE 1-5 one strain gauge indicated wrong values. Calculative corrected values have been parenthesised in table 1.

Table 1. Failure-loads

Test	Left Laminate			Right Laminate		
	$F_{l, \text{left}, \text{max}}$ [kN]	$F_{l, \text{left}, \text{min}}$ [kN]	$\Delta F_{l, \text{left}}$ [kN]	$F_{l, \text{right}, \text{max}}$ [kN]	$F_{l, \text{right}, \text{min}}$ [kN]	$\Delta F_{l, \text{right}}$ [kN]
ZRE 0-1 ¹	54,8	30,7	24,1	54,8	30,7	24,1
ZRE 1-1	61,8	44,4	17,4	61,8	41,2	20,6
ZRE 1-2	50,9	40,5	10,4	47,3	42,2	5,1
ZRE 1-3	48,8	40,5	8,3	54,5	40,7	13,8
ZRE 1-4	51,3	41,6	9,7	55,3	42,3	13,0
ZRE 1-5 ²	51,8	(40,6)	(11,2)	55,1	(41,9)	(13,2)
ZRE 1-6	56,7	41,8	14,9	58,7	41,9	16,8

bold failure of bond between concrete and **this laminate**

¹ no strain gauges were used to estimate the forces between the laminates; forces were divided equally

² a strain gauge gave wrong values

() calculative corrected values

The maximum values of ΔF_1 lay between 10,4 kN for test ZRE 1-2 and 20,6 kN for test ZRE 1-1. One reason for the variation of the force differences ΔF_1 could be variations of tension strength of concrete.

During all bonding tests, first noises could be heard at a load F_1 of about 30 kN. Those noises signify the beginning of crack formation in concrete. Under the higher load (jack 1), this crack formation lead to concrete-wedges (see figure 5) on the interface side.

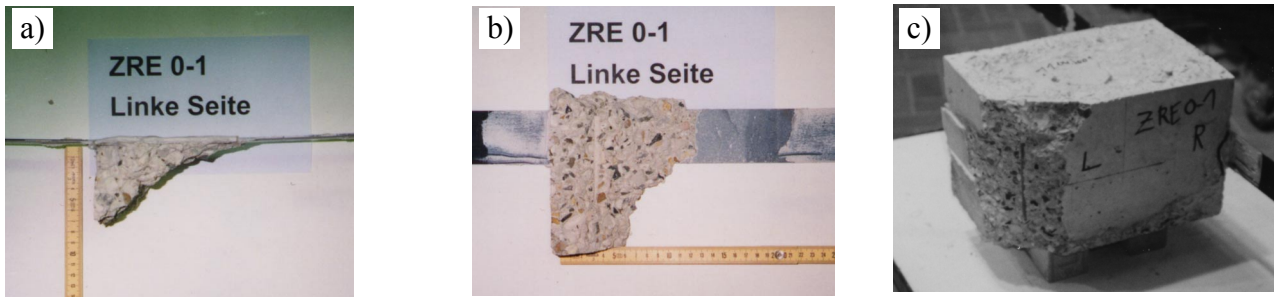


Figure 5. Concrete-wedge at test ZRE 0-1 a) sideview, b) bottomview, c) test specimen ZRE 0-1

Figure 6 and 7 show the distribution of composite strains and shear stresses at the interface between composite and concrete for test ZRE 1-6. The values in the legends notify the forces in the right laminate generated by jack 1 ($F_{1,B}$) and jack 2 ($F_{1,A}$); see figure 2.

As the forces of both jacks are raised equally, the strain gradient forms symmetrically (see figure 6). The maximum values of shear stresses between two strain gauges were calculated with 6 N/mm^2 . As to be expected, the zero-crossing of shear stresses lies in the middle of the bond length. Furthermore, it is remarkable that with increasing load the maximum shear stresses moved from the outside to the centre of the bond length (see figure 6). This was caused by shear deformation of adhesive and by successive destruction of interface between laminate and concrete.

After holding the force $F_{1,A}$ at 40 kN the strain gradients changed significantly. The strains in the laminate at the left side increased at a force of 57,6 kN up to 5,5 %. As expected, the strains in the laminate at the right end of the interface remained the same. At load of 55,1 kN and 57,6 kN the strains in the middle of the interface length increased substantially, too. Shortly before debonding failure between laminate and concrete, the strains decreased remarkably - except for the laminate end loaded with 58,7 kN.

It can be assumed that the shift of shear stresses is caused by preceding destruction of interface between laminate and concrete. The maximum shear stresses amounted to 15 N/mm^2 . Figure 7 illustrates that the zero-crossing of shear stresses shifted from the center of bond length to the area of the interface end with the lower load.

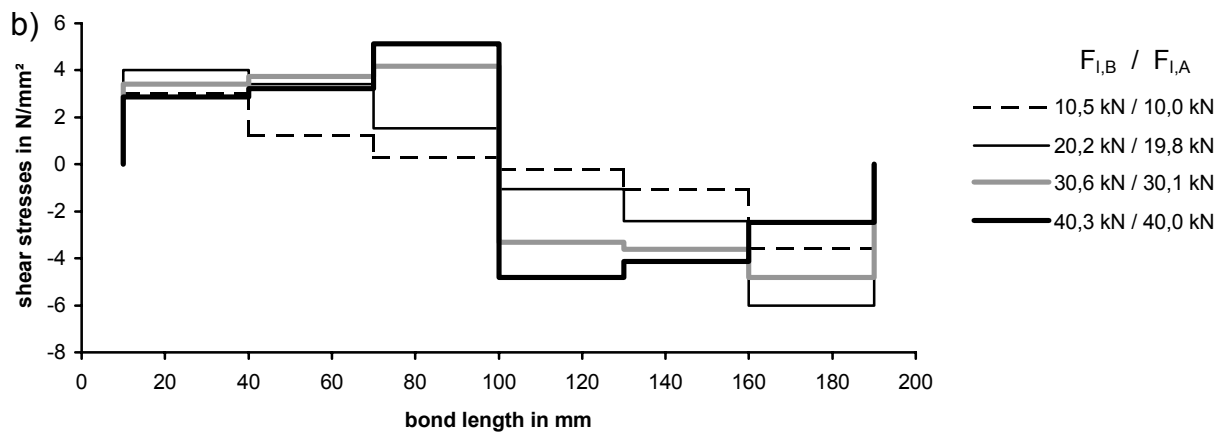
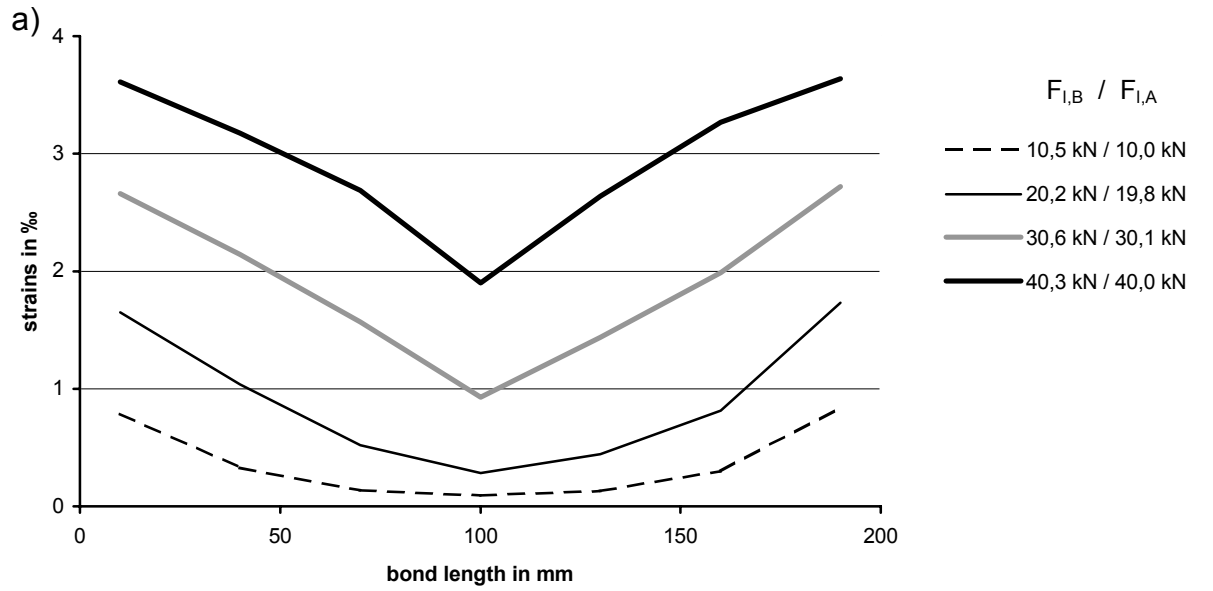


Figure 6. Test ZRE 1-6 (right laminate), a) composite strains and b) shear stress distribution for same load in both jacks

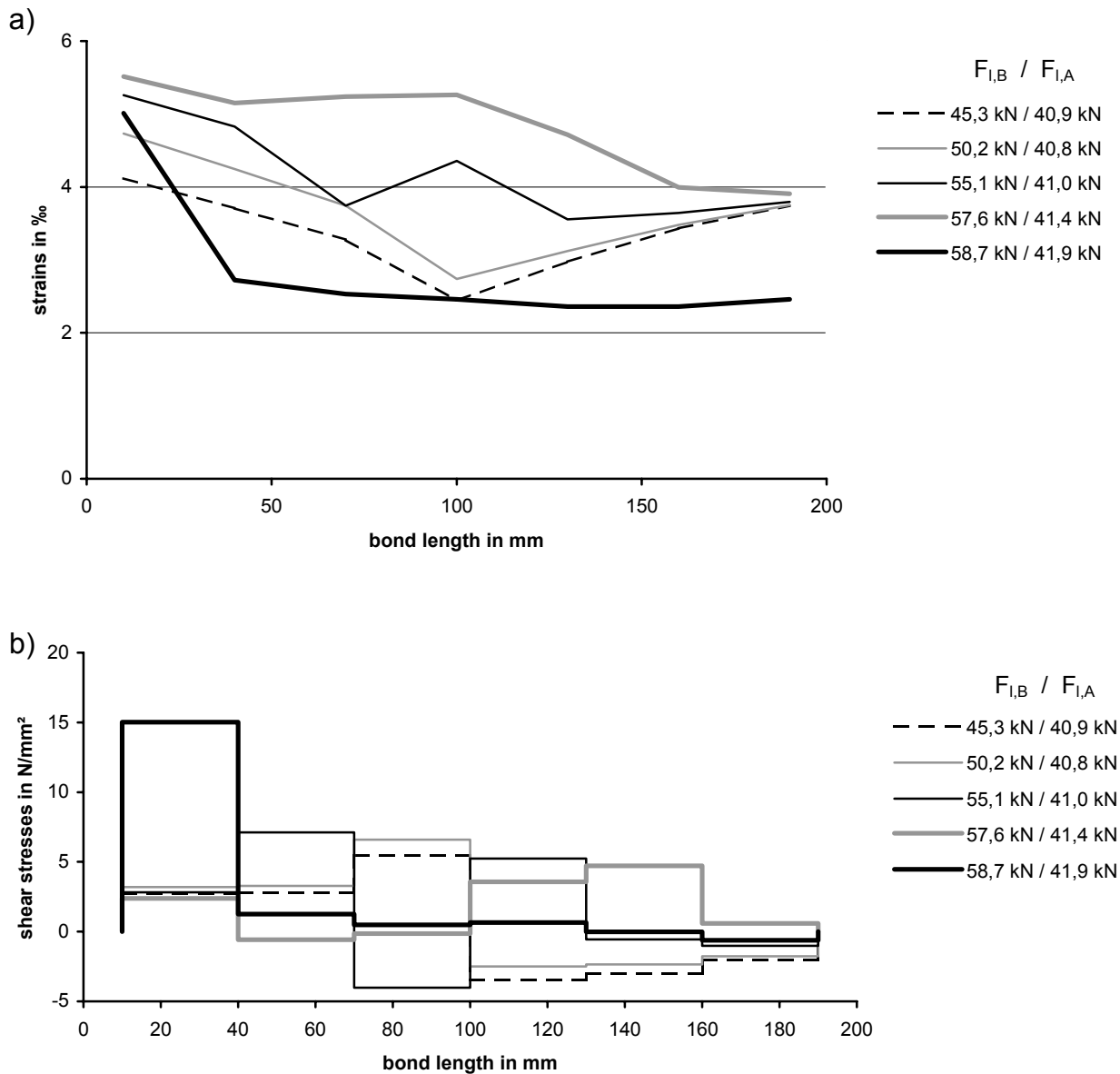


Figure 7. Test ZRE 1-6 (right laminate), a) composite strains and b) shear stress distribution; load of jack 2 held constantly

Finite-Element-Model

For basic verifications of the test results finite-element calculations were carried out with ANSYS 5.7 [9]. Figure 8 shows the 3D element mesh of the test specimen considering vertical symmetry. For concrete and adhesive, solid elements were used. Laminates were modelled by shell elements. Steel reinforcement ($\rho = 5\%$) was 'smeared' over all elements of the concrete block.

Mesh convergence was studied with linear elastic calculations. As a result, maximum and minimum dimensions of the solid elements representing the concrete block were chosen as 12,5mm respectively 6,25mm. The maximum width of the shell element is 25mm, the minimum width 6,25mm. Material parameters are listed in table 2. Young's modulus and tensile strength of concrete were derived from compression strength. The Poisson's ratio is 0,3.

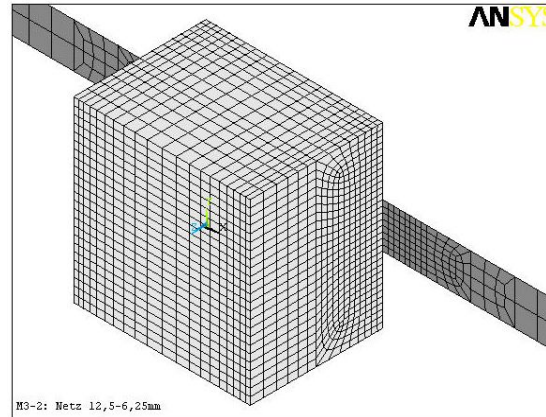


Figure 8. Finite-element model of specimen utilising vertical symmetry

Table 2. Material parameters for finite-element-calculations

	Young's Modulus [N/mm ²]	compression strength [N/mm ²]	tensile strength [N/mm ²]
concrete	35000	47,7	5,0
adhesive	11000	100,0	30,0
laminat	170000	---	2200,0

The calculations were carried out with the following load steps: first, both ends of laminate were successively loaded until 40 kN. Then the load at one end was increased until interruption of calculation. For adhesive thickness of 2,0mm, 3,5mm and 5,0mm ΔF_1 reached values of 17,0 kN, 19,0 kN and 20,5 kN.

The gradients of shear stress on concrete surface over bond length are shown in figure 9 for an adhesive thickness of 2 mm and six load steps. Shear stresses for similar loads until 40 kN form symmetrically. With increasing loads at one end of the laminate, zero-crossing of the curve moves from the middle to the less loaded margin. With increasing loads even maximum stresses move from both sides to the centre.

Figure 10 shows good correspondence between numerical and experimental results for determination of laminate strains over bond length.

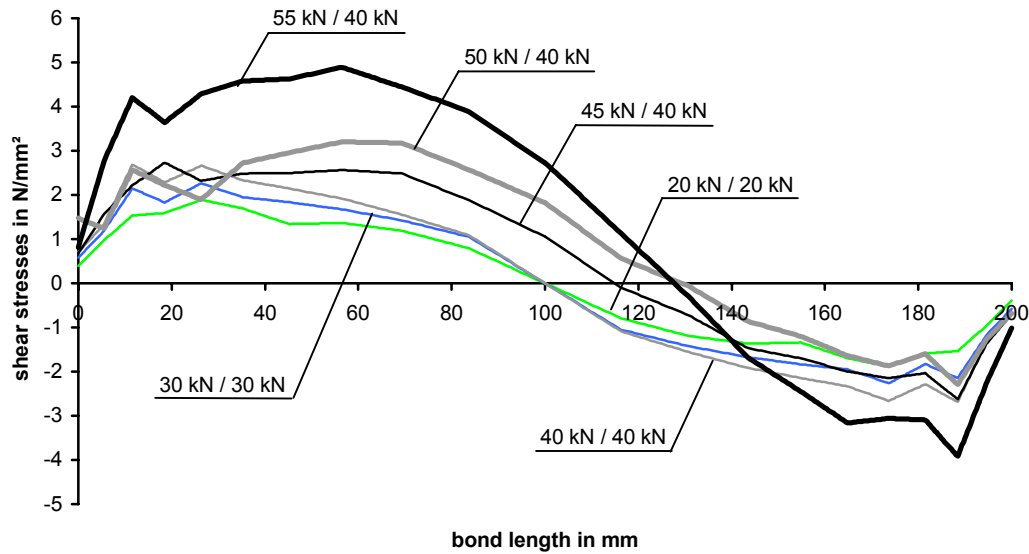


Figure 9. Shear stresses over bond length (adhesive thickness = 2mm)

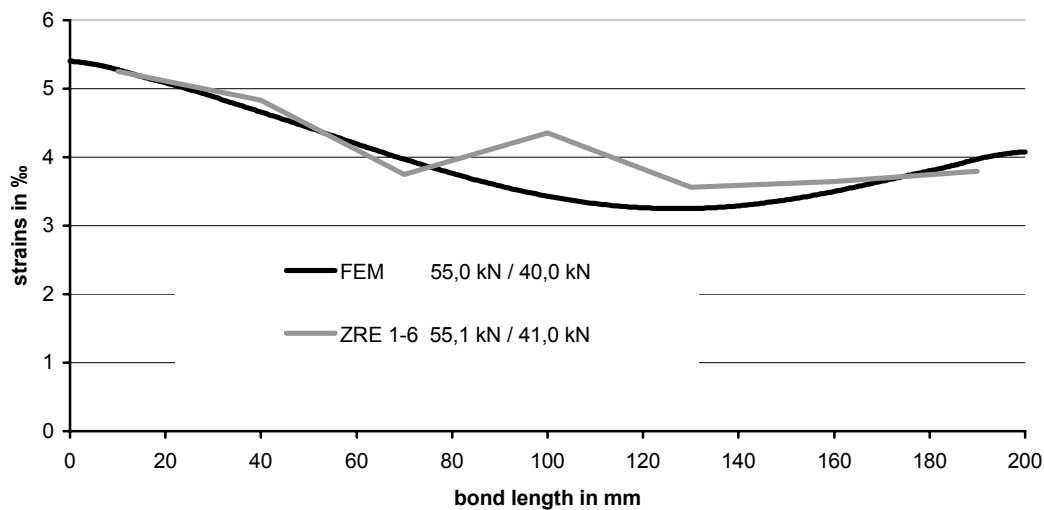


Figure 10. Comparison of strains between FEM-calculation and test ZRE 1-6

Conclusion

It could be shown, that the new developed test set-up is well suited to study bonding behaviour between concrete surface and laminate. The loading procedure and consequently the strain gradient is easy to guide by use of the two jacks. Variation of the test results may be caused by scattering material properties of the concrete. Correspondence between experimental and numerical results could be demonstrated for the development of laminate strains.

For further tests, influence of concrete strength and shear/moment interaction will be studied to develop a well based mechanical model of the debonding phenomenon.

References

1. Willem Jansze (1997), “Strengthening of Reinforced Concrete Members in Bending by Externally Bonded Steel Plates – Design for Beam Shear and Plate Anchorage”, *Doctoral thesis*, Delft University of Technology.
2. Werner Seim, Vistap Karbhari and Frieder Seible (1999), “Nachträgliches Verstärken von Stahlbetonplatten mit faserverstärkten Kunststoffen“, *Beton- und Stahlbetonbau 94:11*, pp. 440-456.
3. Martin Deuring (1993), “Verstärken von Stahlbeton mit gespannten Faserverbundwerkstoffen“, *Dissertation*, Eidgenössische Materialprüfungs- und Forschungsanstalt Dübendorf, Bericht Nr. 224.
4. Hans-Peter Kaiser (1989), “Bewehren von Stahlbeton mit kohlenstofffaserverstärkten Epoxidharzen“, *Dissertation*, Eidgenössische Technische Hochschule Zürich, ETH Nr. 8918.
5. Uwe Neubauer (2000), “Verbundtragverhalten geklebter Lamellen aus Kohlenstofffaser-Verbundwerkstoff zur Verstärkung von Betonbauteilen“, *Dissertation*, Institut für Baustoffe, Massivbau und Brandschutz, TU Braunschweig, Heft 150.
6. S&P Clever Reinforcement Company (2001), “Bemessungsgrundlagen für S&P FRP Systeme“, www.sp-reinforcement.ch.
7. ispo GmbH (1998), “ispo Concretin SK 41 – lösemittelfreier, pigmentierter 2-Komponentenkleber auf Epoxidharzbasis“, *Technisches Merkblatt 657 080*.
8. Heiko Engelhard (2001), “Nachträgliche Verstärkungen mit CFK-Lamellen – Numerische Untersuchungen zum Verbund zwischen Lamelle und Beton“, *Diploma thesis*, Fachgebiet Baukonstruktion und Bauwerkserhaltung, Universität Kassel.
9. ANSYS 5.7.1 (2001), *ANSYS Inc.*, Canonsburg.